

Higgs differential measurements and EFT interpretation in ATLAS

Giuseppe Callea^a for the ATLAS collaboration

^a*University of Glasgow,*

Kelvin Building, University Avenue, Glasgow, UK

E-mail: giuseppe.callea@glasgow.ac.uk

These proceedings present highlights of fiducial and differential cross-section measurements for several Higgs boson production modes and decay channels, offering a unique frame to study its properties at the Large Hadron Collider. The results are compared to Standard Model predictions and in some cases, limits on physics beyond the Standard Model are also extracted in the context of effective field theory models. The measurements use data collected by the ATLAS detector during pp collisions at a centre-of-mass energy of 13 or 13.6 TeV.

12th edition of the Large Hadron Collider Physics Conference (LHCP2024),

3-7 June 2024

Northeastern University, Boston, USA

1. Introduction

Since the Higgs boson's discovery, a vast amount of searches and precision measurements have been conducted at the Large Hadron Collider (LHC) to test the validity of the Standard Model (SM) and search for new evidence that would explain the presence of physics beyond the SM (BSM). The ATLAS experiment [1] has published several measurements covering different Higgs production modes and decay channels for fermions and vector bosons. These analyses have been performed by measuring fiducial and differential cross-sections, using the Simplified Template Cross Section (STXS) method [2] and extracting limits on the coupling modifiers with the kappa-framework [3]. Furthermore, results have been interpreted within the Effective Field Theory (EFT) framework of the SM, which provides a model-independent approach to parameterise the effects of BSM theories that may exist at high energy scales (Λ). This contribution summarises recent fiducial and differential measurements, along with EFT interpretations, using Run2 (2015-2018) and early Run3 (2022) data collected with the ATLAS detector.

2. $H \rightarrow WW$ fiducial and differential cross-section measurements

The $H \rightarrow WW$ decay mode has a good branching ratio but suffers from a degraded resolution in the W -candidate reconstruction due to the neutrino's elusive nature, when the W boson decays leptonically. Differential cross-sections have been studied in the gluon-gluon fusion (ggF) [4] and vector boson fusion (VBF) [5] production modes at 13 TeV in the $e\nu\mu\nu$ final state. Single differential cross-sections have been measured as a function of many variables sensitive to the production kinematics and the dilepton system's spin structure, like $\cos\theta^* = |\tanh(\Delta\eta_{ll}/2)|$ [6], where $\Delta\eta_{ll}$ is the lepton pseudorapidity difference. In the ggF case, double-differential cross-sections have been measured as a function of kinematic variables and jet multiplicity N_{jet} . Figure 1(a) shows the double-differential cross-section as a function of $\cos\theta^*$ and jet multiplicity. The results are in agreement with the SM prediction within uncertainties. Figure 1(b) shows the measured fiducial cross-section for the $H \rightarrow WW$ process in the VBF production mode. Predictions at NLO or LO with parton shower overestimate the measured cross-section by a factor 15-28%, but they are compatible at the level of approximately 1σ . The parton-level fixed-order calculation of VBFNLO@LO is higher than the other predictions by 24%.

3. Combination of $H \rightarrow ZZ$ and $H \rightarrow \gamma\gamma$ fiducial cross-sections at 13 and 13.6 TeV

The $H \rightarrow ZZ$ in the four-lepton (4l) channel and $H \rightarrow \gamma\gamma$ decay channels offer excellent signal resolution but low event counts. The ATLAS collaboration performed a combination of these two channels at the centre-of-mass energies of 7, 8, 13 [7] and 13.6 TeV [8], with the latter providing the most precise measurement on the total Higgs cross-section: $\sigma(pp \rightarrow H) = 58.2 \pm 8.7$ fb at $\sqrt{s} = 13.6$ TeV, in agreement with the SM prediction of 59.9 ± 2.6 fb. Differential cross-sections as a function of the Higgs p_T are measured with 20-30% (60%) precision up to 300 (350-600) GeV. Figure 2(a) shows the measured values of $\sigma(pp \rightarrow H)$ as a function of the centre-of-mass energies. Differential measurements in the Higgs p_T can be used to study the Higgs Yukawa couplings with the b - and c -quarks. Any modifications to their coupling strength will result in changes to the overall

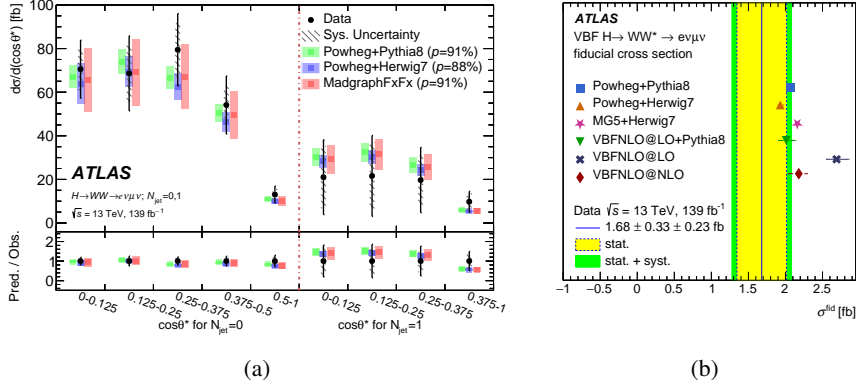


Figure 1: (a) Double-differential cross-section as a function of $\cos\theta^*$ and N_{jet} for the ggF $H \rightarrow WW$ decay mode [4]. (b) The measured fiducial cross-section for the $H \rightarrow WW$ process in the VBF production mode [5]. Both results have been compared to the SM predictions.

Higgs production cross-section and the p_T shape, and to the $H \rightarrow ZZ$ and $H \rightarrow \gamma\gamma$ branching ratios. Combined measurement of the $H \rightarrow ZZ$ and $H \rightarrow \gamma\gamma$ decays with the $VH(b\bar{b})$ [9] and $VH(c\bar{c})$ [10] measurements at $\sqrt{s} = 13 \text{ TeV}$ provides tight constraints on the Yukawa coupling modifiers for b - (k_b) and c -quarks in the kappa-framework (k_c). Figure 2(b) shows the contours for the k_b and k_c parameters from a simultaneous fit to the Higgs p_T fiducial cross-section for the $H \rightarrow ZZ \rightarrow 4l$ and $H \rightarrow \gamma\gamma$ decays and to multivariate discriminants used to identify the $VH(b\bar{b}/c\bar{c})$ channels. This combination provides updated constraints on k_c of $[-2.47, 2.53]$ at 95% Confidence Level (CL), representing the most stringent limits to date on this parameter.

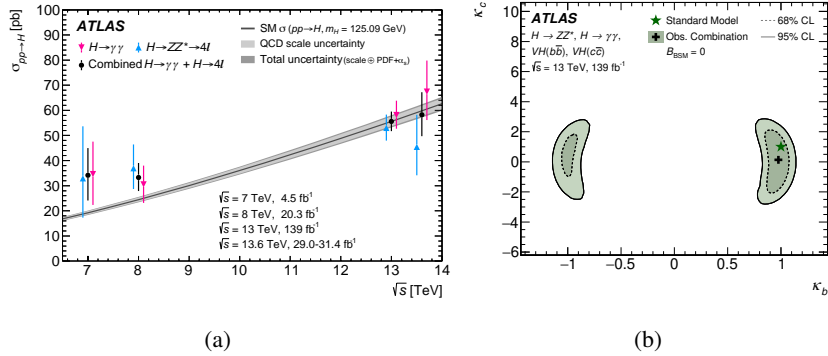


Figure 2: (a) Higgs cross-section measured at the centre-of-mass of 7, 8, 13 and 13.6 TeV and compared to the SM predictions [8]. (b) 2D negative log likelihood contours for the k_b and k_c parameters for the $H \rightarrow ZZ \rightarrow 4l$ and $H \rightarrow \gamma\gamma$ combinations with the $VH(b\bar{b}/c\bar{c})$ decays, assuming that the branching ratio of the BSM particles is equal to 0 ($B_{\text{BSM}}=0$) [7].

4. EFT interpretations

EFT interpretations provide an elegant language to encode modifications to SM properties induced by BSM theories. In this framework, the effects of BSM dynamics at the Λ energy scale (e.g., 1 TeV), well above the electroweak scale, can be parameterised at low energies in terms of higher-dimensional operators built up from the SM fields and respecting its symmetries such as gauge invariance. The ATLAS collaboration interprets the result as constraints on the Wilson coefficients, which correspond to operators that either directly or indirectly impact Higgs boson couplings to SM particles. The cross-section predictions for a specific process are estimated as the sum of the SM, the interference between the BSM and SM operators (linear), and the BSM cross-section (quadratic) terms.

4.1 EFT interpretation of combined STXS measurements

A recent combination of different production modes and decay channels [11] probed by ATLAS measurements has been used to evaluate limits on many Wilson coefficients in the EFT interpretation. Figure 3 shows the limits on the Wilson coefficient for the case where only linear contributions of the EFT to the cross-sections are considered, in terms of single Warsaw basis c_j coefficients and a linear combination of some of them e_k . A linear combination was chosen to achieve both fit stability and fit-parameter interpretability. The results show good agreement with the SM. Observed uncertainties are generally smaller than the expected ones. This is because the assumed Higgs boson width is smaller than its SM expectation value and it is mostly driven by a high observed value of the Yukawa coupling modifiers for $H \rightarrow b\bar{b}$ (c_{bH}), which corresponds to a reduced value of the $H_{b\bar{b}}$ decay width, $\Gamma^{H \rightarrow b\bar{b}}$. Limits considering the quadratic term of the EFT Lagrangian are also evaluated and provide more stringent constraints on Wilson coefficients for a mass scale of 1 TeV.

4.2 EFT based on differential measurements

Coefficients of EFT operators can alternatively be constrained from fiducial cross-section measurements which are explicitly unfolded to the particle level. The finer granularity of kinematic regions defined in differential measurements offers an advantage in the analysing power of differential distributions compared to STXS measurements. On the other hand, this aspect is counteracted by the inclusive treatment of Higgs boson production processes, which are modelled separately in the STXS approach. In this case, constraints on the anomalous Higgs coupling to gluons and top quarks are set from the observed Higgs p_T in $H \rightarrow ZZ$ and $H \rightarrow \gamma\gamma$ events at 13 TeV. The $e_V^{[1,2,3]}$ eigenvectors are built from a rotation of Wilson coefficients c_{HG} , c_{tG} and c_{tH} so they can be probed simultaneously. Figure 4 shows the observed 68% CL intervals on the $e_V^{[1,2,3]}$ parameters in the EFT linearised model using either STXS or fiducial p_T -differential cross-section measurements. As expected, the latter shows less constraining power than the STXS measurements, as they probe the distribution of a single observable inclusively in production mode.

5. Summary

The ATLAS collaboration has performed a wide range of precision measurements on many Higgs boson properties by extracting fiducial and differential cross-sections at different centre-of-mass energies and interpreted the results with the STXS and the kappa frameworks. The results are in good agreement with the SM predictions. Many of these measurements have been combined and interpreted in the EFT scenario, providing stringent constraints on the Wilson coefficients. We look forward to having more precision measurements with the LHC Run3 data.

References

- [1] ATLAS Collaboration, JINST (2008) 3, S08003
- [2] LHC Higgs Cross Section Working Group, CERN-2017-002 (2017)
- [3] S. Heinemeyer, C. Mariotti, G. Passarino, R. Tanaka et al., CERN-2013-004 (2013)
- [4] ATLAS Collaboration, Eur. Phys. J. C (2023) 83, 774
- [5] ATLAS Collaboration, Phys. Rev. D (2023) 108, 072003
- [6] A.J. Barr, JHEP 02 (2006) 042
- [7] ATLAS Collaboration, JHEP 05 (2023) 028
- [8] ATLAS Collaboration, Eur. Phys. J. C (2024) 84, 78
- [9] ATLAS Collaboration, Eur. Phys. J. C 81 (2021), 178
- [10] ATLAS Collaboration, Eur. Phys. J. C 82 (2022), 717
- [11] ATLAS Collaboration, arXiv:2402.05742